IPBI-TN-2004-7
July 13, 2004

Rough Layout and Rate Estimate for Beam Test in SLAC ESA of Synchrotron Radiation Detector Prototypes for LC Beam Monitor

R. Arnold
UMass, Amherst, MA 01003

E. Torrence
University of Oregon, Eugene OR

Introduction

This note gives a rough experiment layout and counting rate estimate for the beam test of a proposed synchrotron light beam monitor for LC spectrometry. The idea for this detector is documented in Ref [1]. The proposal for a beam test SLAC Proposal T-475(June 2004) can be found at http://www.slac.stanford.edu/xorg/lcd/ipbi/documentation.html.

The method proposed for the LC detectors is similar to that employed by the WISRD spectrometer[2] at the SLAC Linear Collider/SLD interaction region. The idea is to generate two stripes of synchrotron light, one up-beam and one down-beam of a well know bend magnet somewhere in the extraction line system of the LC. Measurements of the positions and shapes of the two synchrotron stripes, together with precise knowledge of the geometry and the field in the bend magnet, can be used to determine many properties of the spent beam from the Linear Collider. A main goal is to determine the beam energy from the distance between the stripes. Other interesting features would be to extract information about the spectrum of the spent beam, and therefore information about the e+e- collision, from the shapes of the synchrotron stripes. The purpose of the proposed test is to begin testing candidate detector technologies in a synchrotron beam and learn how to design a detector for the LC. This note gives a very crude estimate of the expected counting rate in the proposed detectors.

Experiment Layout

A sketch of the main features of the basic layout is shown in Fig 1. The synchrotron light will be generated in a wiggler magnet aligned at 0.005 rad to the main beam line. The incident beam will be first deflected horizontally in a bend magnet B1, passed through the vertical wiggler, and then after the wiggler it will be deflected back in B2 offset and parallel to the original direction so it can exit the ESA hall into Beam Dump East. The synchrotron stripe from the wiggler will proceed forward and be extracted from the vacuum system downstream at some point conveniently far enough away from the electron beam to allow space for the exit window and the detectors. This arrangement would test one leg of the system proposed for the LC, and is mainly aimed at understanding the performance of the detectors. A second leg with a calibrated bend magnet between would be needed to measure the beam energy.

Some considerations in choosing the geometry of the layout are:

- The space required by the setup is partly constrained by available room in the SLAC

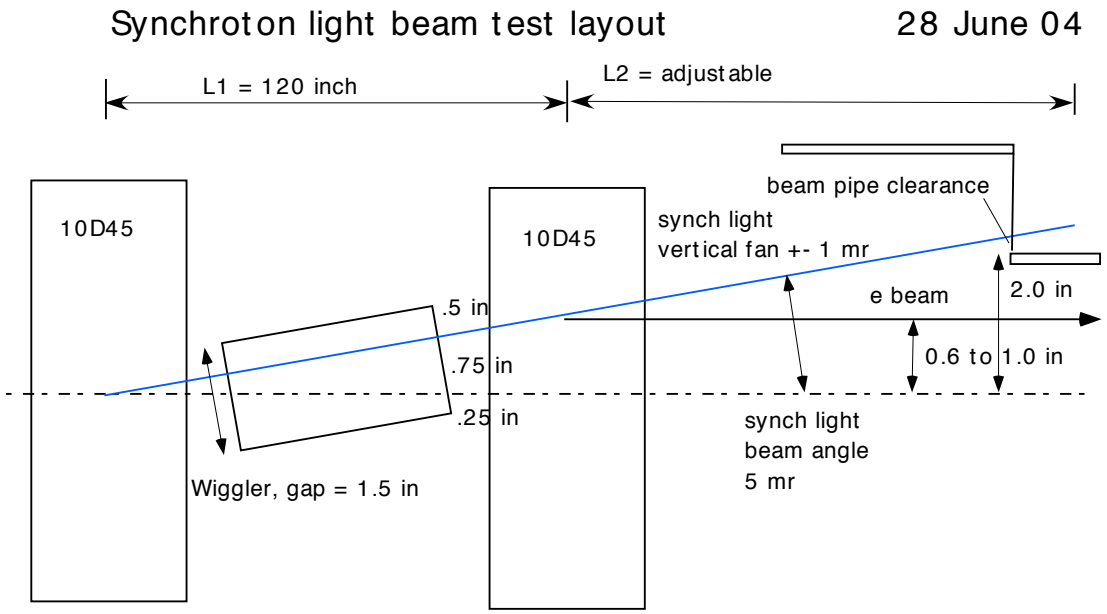

L2	L_tot (inches)	Pipe Clearance
480	600	1.0
680	800	2.0
880	1000	3.0

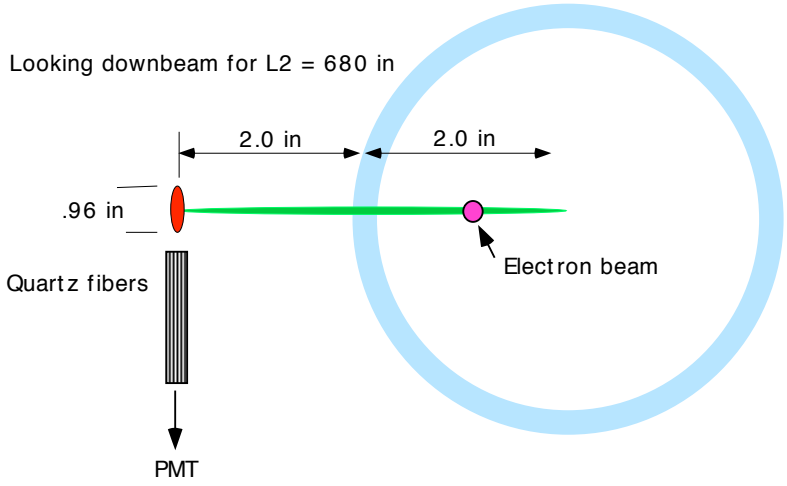

Figure 1: Top figure: schematic layout (not to scale) of the proposed synchrotron stripe detector test in SLAC ESA. Bottom figure: looking down beam at a projection in x vrs y of the synchrotron stripes from the wiggler (vertical red blob) and the bend magnets (horizontal green blob) and the exit beam pipe at the location of the fiber detectors for the case of $L2 = 680$ inches in the top figure.

ESA, and needs to be kept to a reasonably short length. The length required for the bends and wiggler is partly determined by the length of the bends, and by the space needed for coils, flanges and access. The length 120 inches shown in Fig 1 is estimated for the 10D45 magnets, and the 10D90s would be a bit longer. This length, together with the bend angle, determines the exit beam offset and thus the radius required for the exit beam pipe.

- The bend angle in the first bend is constrained to small values by the need to permit both the bent beam and the straight-ahead beam through the 1.5 inch wide pole gap of the wiggler (minus vacuum chamber walls). Allowing clear passage for the straight-ahead beam facilitates operations with the bend magnets off.

- The bend angle is constrained on the small side by the need to extract the synchrotron beam from the beam pipe in a reasonably short distance down-beam from the wiggler. The exit beam pipe is set at 2 inch radius to limit background from upstream scattering of beam halo. The synchrotron stripe must clear the beam pipe with some room to spare to permit installation of the fiber detectors. The pipe radius and the synchrotron clearance, together with the 5 mr bend angle determines the distance from B2 to the detectors. Three cases are shown in a table in Fig 1. For the rate estimates the middle value for L2 = 680 inches corresponding to clearance of 2 inches is used. This choice affects the fraction of bend spray that could intercept the detectors.

More study with simulations of signal and background rates will be needed to choose the final values for the bend angle, exit pipe size, synchrotron clearance and other parameters, but they will be similar to the ones shown in Fig 1.

The proposed detector will be made of various sizes of quartz fibers arranged in various orientations to sample the stripe from the wiggler and connected to a multi-anode PMT. The detector works by registering light in the PMT from Čerenkov light made in the quartz from recoil electrons (and a few positrons) generated in the quartz by the synchrotron photons. The purpose of this note is to estimate the counting rate in such a detector using rough numbers for the synchrotron flux produced in the wiggler and crude estimates of the response of the quartz/PMT system to those photons. For this estimate we assume the fibers are 0.6 mm thick oriented vertically side-by-side with the center of the bunch centered on the wiggler stripe.

An important difference between this test and the proposed LC arrangement is that the beam energy in the test will be of the order of 28 GeV, much lower than the many hundreds of GeV at the LC. This results in synchrotron light spectra which are lower in energy than those at the LC, and a main point of this estimate is to show that such a low energy beam is still useful for a test.

Another point to be studied is how to optimize the geometry of the test. One question is which of the available bend magnets would be best. The current best choices are either 10D45 or 10D90 magnets from the original SPEAR ring at SLAC. They have gaps 10 inches wide and 2.5 inches tall, and are 45 and 90 inches long respectively. Longer magnets extend the size of the total layout, and being heavier, are somewhat more costly to mount. However we shall see that longer magnets give much less background synchrotron light in the detectors, and are probably preferred.

The wiggler magnet to be used is also from the early history of SPEAR and is documented in Ref [3]. It is oriented to bend electrons vertically giving a vertical synchrotron stripe at the detectors.

Parameters of Čerenkov Light in Si and Synch Light in the Bend Magnets
Electrons at Čerenkov threshold in quartz have:

$$\beta = 1/n \quad = 0.6859 \tag{1}$$
$$\text{total energy} \quad = 0.7022 \text{ MeV} \tag{2}$$
$$\text{kinetic energy} \quad = 0.2269 \text{ MeV} \tag{3}$$

Calculate the critical energy E_c in the wiggler from $E_c = 0.0665$ B(kG) E^2 (GeV). Using 17 kG max pole field and beam energy $E_0 = 28$ GeV gives $E_c = 0.886$ MeV for the wiggler. In the actual wiggler field some of the path length is at lower than the maximum field, so part of the photon spectrum will have lower critical energies.

Consider two possible bend magnets, 10D45 (length = 45 inch) and 10D90 (length = 90 inch) and bend angle of 0.005 rad. This gives bend total BL = 4.66 (kG-m). Field and critical energy in the bends is

$$10D45 \quad = 4.087 \text{ kG} \qquad E_c45 \quad = 0.213 \text{ MeV} \tag{4}$$
$$10D90 \quad = 2.044 \text{ kG} \qquad E_c90 \quad = 0.106 \text{ Mev} \tag{5}$$

To estimate synchrotron photon rates we use some cool notes from Hobey DeStaebler from his work on backgrounds in PEPII and BaBar. These were published in the Appendix A of Ref [4], included below. Hobey gives lots of useful formulas and some tables. The most important is a formula for the average number of photons emitted along a circular arc in a bend magnet

$$< n >= 0.6181 \text{ B(kG)L(m) photons/electron} \tag{6}$$

and Table A.1 showing the fraction of the number of photons and the fraction of the energy carried by photons above E/E_c for various E.

The main parameters for the wiggler are: BL = 0.831 kG-m for one half pole at 17 kG full field (practical maximum operating value scaled from 20 kG field given in SLAC PUB 2289). The wiggler has 6 full poles. The synchrotron flux from the wiggler makes a vertical stripe at the fiber detector with total flux of

$$< n > \quad = 0.6181)(2)(0.831)(6) \tag{7}$$
$$= 6.19 \text{ photons/electron} \tag{8}$$

The horizontal stripe of synchrotron photons from the bend magnets acts as a background in the fiber detectors. If the fibers intercept the photons from the bend, they generate uninteresting rate that confuses the measurement of the position and shape of the vertical wiggler stripe. At the LC the fiber detector is planned to be located above or below the bend stripe to avoid that background. Here in the test beam the photons from the bend stripe

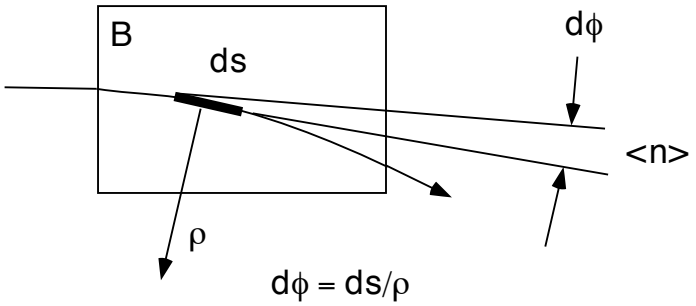

Figure 2: Notation used in Appendix A for synchrotron photons from a segment of a circular arc bend. Formulas for photon flux are integrated over the angular distribution perpendicular to the bend plane.

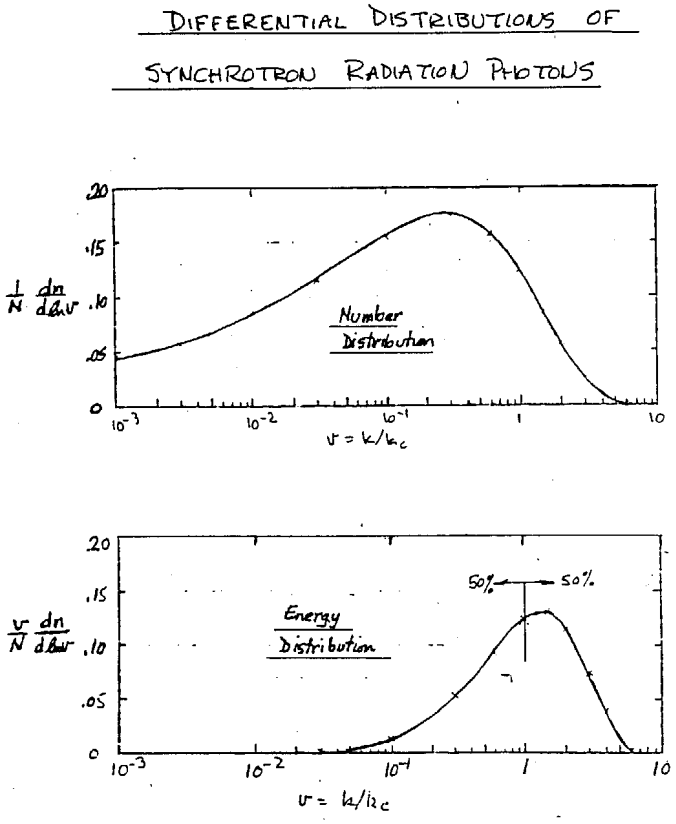

Figure 3: Distributions of synchrotron photons vrs energy (k is the photon energy, k_c is the critical energy). Top fig: number distribution of photons; bottom fig: energy distribution carried by the photons. From Hobey DeStaebler, priv comm. Values plotted are from tables by R. A. Mack, Ref. 55 in Appendix A.

are sufficiently low in energy that they do not present a serious background because they make recoil electrons in the quartz mostly below Čerenkov threshold. As we show below, the 10D90 magnets are better in this respect, because the bend field for a given bend angle is lower than for the 10D45 magnets, and the synchrotron critial energy is lower. The number of photons in the full bend stripe is same for 10D45 and 10D90 (same BL)

$$< n > = (0.618)(4.66\text{kG} - \text{m})(2 \text{ bends}) \quad (9)$$

$$= 5.76 \text{ photons/electron} \quad (10)$$

Čerenkov Signal in Quartz from Recoil Comptons above Cherenkov Threshold

Using Compton formulas for max recoil energy T_{max} and looking at pictures of distributions for Compton scattering in text books (see Fig 5 and 6), we estimate that photons above 0.4 MeV can make recoil electrons with kinetic energy above the 0.2 MeV Čerenkov threshold in quartz. For photons in the range 0.8 to 1.0 MeV (the most useful ones we have) the fraction of recoil Compton electrons above 0.2 MeV is 0.8 to 0.9. We use 0.8 in the following estimates. Using Table A.1 from Appendix A., we get the fraction of synchrotron photons above 0.4 MeV for each source (wiggler, 10D45, 10D90)

For the wiggler we asume all the photons made impinge on the detector. This corresponds to putting the fibers to cover the full stripe from the wiggler. In this position they would also intercept a small portion of the tip of the synchrotron stripe from the bends. We can do this if the synchrotron photons from the bends are low enough energy so as to not produce much signal in the fibers, which is probably the case (see below). If the fibers have to be pulled up or down to stay out of the plane of the bend stripe, then the rates from the wiggler will be reduced accordingly.

For the bends only a fraction of the stripe hits the detector. For the case of two bends, the bend stripe is only on one side of the incident beam. We estimate the fraction of the bend stripe intercepted by the detectors to be:

0.08 = (0.8 cm detector width in the stripe) / (10 cm stipe width)

The interaction of synchrotron photons in the fibers is dominated by Compton scattering, with a small amount of pair production for the higher energies (See Fig. 4). The attenuation coefficient (Particle Data Book) for 0.5 to 2 MeV photons in Si is approximately $t_{atten} = 20$ (g/cm^2). The quartz fiber thickness is $t = 0.6$ (mm) and density is $\rho = 2.33$ (g/cm^3), so $t\rho =$ 0.14 (g/cm^2). The transmission of photons through the fibers is then $e^{-(\frac{t\rho}{t_{atten}})} = 0.99302$. The fraction of synchrotron photons that interact in the fibers is 0.007.

Note: the recoil Compton electrons are produced mostly at a range of fairly wide angles to the incident photons (see Fig. 5), and they have low kinetic energy and fairly short ranges (0.1 to 0.8 g/cm^2). They will straggle in the fibers producing Čerenkov light as long as they remain above 0.2 MeV. Any material in front of the fibers, such as the vacuum exit window or any preradiator, will attenuate the low energy photons, mostly by photo electric effect, but will not significantly enhance the number of recoil electrons through the fibers because the cross section is dominated by Compton scattering that produces recoil electrons at wide angles and is mostly below the pair threshold.

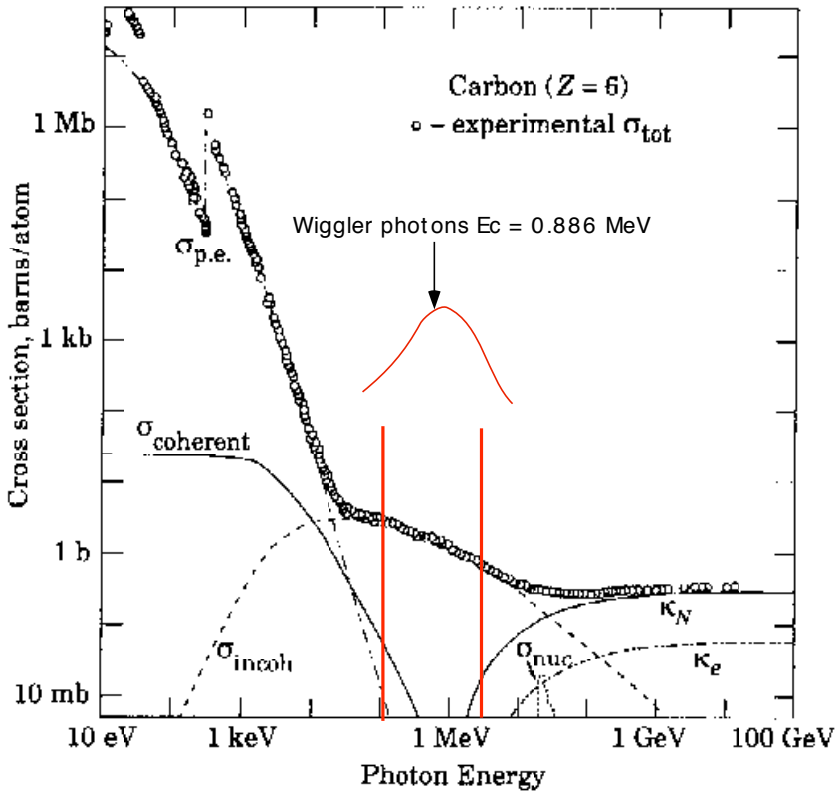

Figure 4: Photon cross sections in carbon, similar to Si (Particle Data Book). Also indicated is a sketch of the approximate distribution of the synchrotron photons from the wiggler with critical energy $E_c = 0.886$ MeV. The interaction cross section is dominated by Compton scattering ($\sigma_{incoherent}$).

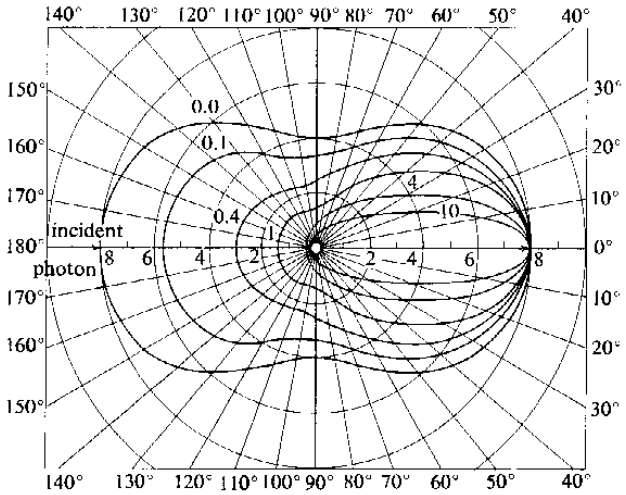

Figure 2-27 Polar diagram of the differential cross section per electron for Compton scattering. Curves labeled according to $\alpha = h\omega/mc^2$ of incident photon. Unit of $d\sigma/d\omega = 10^{-26}$ cm^2 sr^{-1}.

Figure 5: Angular distribution of Compton scattered photons, from "Nuclei and Particles", p.55, E. Segre, Benjamin (1965). In our useful photon range 0.5 to about 2 MeV ($\alpha \simeq 1$ to 4) the cross section is dominated by photons scattered at forward angles with recoil electrons at wide angles.

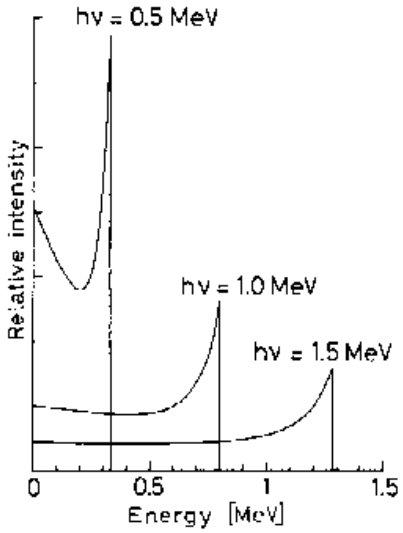

Fig. 2.24. Energy distribution of Compton recoil electrons. The sharp drop at the maximum recoil energy is known as the *Compton edge*

Figure 6: Energy distribution of Compton recoil electrons, from "Techniques for Nuclear and Particle Physics Experiments", p.57, W. R.Leo, Springer-Verlag (1994). For photon energies above 0.8 MeV about 0.8 to 0.9 of the recoil electrons are above 0.2 MeV Čerenkov threshold in quartz.

The final number needed to calculate counting rates is the efficiency for a single recoil electron in a fiber to make a signal in the PMT. This is impossible to calculate by hand as it involves all the Compton and Čerenkov angles, absorption and propagation of light in the fibers, PMT efficiency etc. For the electron detection efficiency we use the number obtained in preliminary work for a proposal for LC detector development Ref [5]. Using a cosmic ray telescope of scintillating fibers on each side of a set of quartz fibers, the efficiency for observing a photon in the PMT from the quartz per cosmic ray was found to be 0.5 %. One photon in the PMT is not much, and cosmics are minimum ionizing particles at many MeV that make Čerenkov light over their full path in the fibers, so this may be an over estimate of the useful efficiency of the relatively low energy recoil Compton electrons.

Summarizing, the factors for rates in the fiber detector from the wiggler are:

- beam energy $E_0 = 28$ GeV and intensity $I = 10^{11}$ e/pulse
- synchrotron flux from wiggler – 6.19 photons/electron
- fraction above 0.4 MeV that can make Čerenkov light (from Hobey's Table A.1) = 0.18
- fraction that make Compton interactions in fibers = 0.007
- fraction of Compton interactions that make recoil above 0.2 MeV = 0.8
- efficiency for one Compton electron to make a signal in the PMT = 0.005

These factors yield for the total detected counts in all fibers from the wiggler

$$N \text{ detected } = (6.19 \times 10^{11})(0.18)(0.8)(0.007)(0.005) \quad (11)$$

$$= 3.11 \times 10^6 \text{ electrons/pulse} \quad (12)$$

Similary, we can estimate rates in the fibers from the bend stripe.

- synchrotron flux 5.76 photons/electron from two bends
- fraction above 0.4 Mev (from Hobey's Table A.1) = 0.02 (10D45) = 0.002 (10D90) The lower bend field and lower critical energy in the 10D90 reduces the rate of high energy photons by a factor of roughly 10 compared to the 10D45. This is good.
- fraction of Compton ineractions that make recoil above 0.2 MeV = 0.8
- fraction of bend stripe hitting the detector = 0.08
- fraction incident that make Compton in fibers = 0.007
- efficiency for one Compton electron to make signal in PMT = 0.005

The total detected counts from the bends is then:

$$2.58 \times 10^4 \text{ electrons/pulse(10D45)} \quad (13)$$

$$2.58 \times 10^3 \text{ electrons/pulse(10D90).} \quad (14)$$

This yields ratios of signal/background: 120 (10D45) and 1200 (10D90)

There are lots of crude approximations here, but its a start.

APPENDIX A

FORMULAS FOR SYNCHROTRON RADIATION

11.1. Bend Magnets

These formulas pertain to electrons in circular motion.[53,36,54] The average number of photons radiated in path length ds is

$$\frac{dn}{ds} = \frac{5}{2\sqrt{3}} \frac{\alpha\gamma}{\rho} , \qquad (A.1)$$

$$\begin{aligned} n &= \langle n \rangle = 20.6 \text{ E(GeV)}\phi \text{ (rad)} \\ &= 0.618 \; B \; L(\text{kG} - \text{m}) . \end{aligned} \qquad (A.1a)$$

The spectrum is a universal function of the characteristic energy

$$k_c = \frac{3}{2} \gamma^3 \frac{\hbar c}{\rho} = \frac{3}{2} \frac{\gamma^3}{\alpha} \frac{r_e}{\rho} mc^2 , \qquad (A.2)$$

$$= 2.22(\text{keV}) \left(\frac{E}{10 \text{ GeV}} \right)^3 \left(\frac{1 \text{ km}}{\rho} \right) , \qquad (A.2a)$$

$$= 6.66(\text{keV}) \left(\frac{E}{10 \text{ GeV}} \right)^2 \left(\frac{B}{1 \text{ kG}} \right) . \qquad (A.2b)$$

The normalized photon energy is

$$v = \frac{k}{k_c} . \qquad (A.3)$$

The normalized number distribution of the photons is

$$\frac{1}{n} \frac{dn}{dv} = \frac{3}{5\pi} \int_v^\infty K_{5/3}(y) \, dy , \qquad (A.4)$$

$$\approx 0.4105 \, v^{-2/3} (1 - 0.8438 \, v^{2/3} + 0.0 v^{4/3} + \ldots) \quad v << 1 ,$$

$$\approx \frac{3}{5\sqrt{2\pi}} \frac{e^{-v}}{\sqrt{v}} \left(1 + \frac{55}{72} \frac{1}{v} - \frac{0.9791}{v^2} + \ldots \right) \qquad v >> 1 .$$

Half of the energy is carried above $v = 1$, by only 8.7% of the photons. Half of the photons are above $v = 0.078$.

For convenience, Table A.1 lists some values for the spectrum (*A*.4) and its integrals.[55] f_N is the fraction of the number of photons above v, and f_E is the fraction of the energy carried by photons above v.

v	$dn/n\ dv$	f_N	f_E
0.01	8.50	0.7381	0.9979
0.03	3.91	0.6277	0.9912
0.1	1.562	0.4628	0.9502
0.2	0.863	0.3483	0.9052
0.3	0.584	0.2775	0.8485
0.5	0.333	0.1896	0.7369
1.	0.1244	0.08677	0.5000
2.	0.0288	0.02326	0.2150
3.	0.00818	0.00703	0.0886
5.	0.00081	0.000737	0.0142

Table A.1. *Photon energy spectrum v for electrons in circular motion, normalized to the critical energy. f_N is the number of photons above v and f_E is the fraction of energy carried by photons above v*

The energy loss per electron has average value

$$\langle U\rangle = \langle n\rangle\langle k\rangle \qquad (A.5)$$

$$= 1.267\ (\text{keV})\left(\frac{E}{10\ \text{GeV}}\right)^2\left(\frac{B}{1\ \text{kG}}\right)^2 L(\text{m}) \quad (A.5a)$$

$$= 140.8\ (\text{keV})\left(\frac{E}{10\ \text{GeV}}\right)^4\left(\frac{1\ \text{km}}{\rho}\right)\phi(\text{rad}) (A.5b)$$

and variance

$$\text{var}(U) = \langle (U-\langle U\rangle)^2\rangle = \langle n\rangle\langle k^2\rangle \qquad (A.6)$$

$$= 11.17(\text{keV}^2)\left(\frac{E}{10\ \text{GeV}}\right)^4\left(\frac{B}{1\ \text{kG}}\right)^3 L(\text{m}) (A.6a)$$

$$= 414\ (\text{keV}^2)\left(\frac{E}{10\ \text{GeV}}\right)^7\left(\frac{1\ \text{km}}{\rho}\right)^2 \phi(\text{rad})\,(A.6b)$$

where $\langle v \rangle = 0.3079$ and $\langle v^2 \rangle = 0.4074$ have been used.[53] Equation (*A*.6) arises because var(U) depends on fluctuations in n as well as in k; a Poisson distribution for n has been used. The angular distribution of the radiated energy integrated over all k is

$$\frac{1}{U}\frac{dU}{dw} = \frac{21}{32}\frac{1+(12/7)w^2}{(1+w^2)^{7/2}}, \quad -\infty \le w \le \infty, \quad (A.7)$$

$$w = \gamma\psi, \quad (A.7a)$$

where ψ is the angle perpendicular to the bend plane. For some cases of heating by bend SR, it is useful to have an approximate expression for the full double differential distribution. For fixed v, approximate the w dependence with a Gaussian. Then

$$\frac{1}{U}\frac{dU}{dv\,dw} \approx \frac{1}{U}\frac{dU}{dv}\cdot\frac{1}{\sqrt{2\pi}\sigma_w}\exp\left\{\frac{-w^2}{2\sigma_w^2}\right\}, \quad (A.8)$$

$$\sigma_w \approx \left(\frac{0.363}{v}\right)^{0.44}. \quad (A.9)$$

This approximation is reasonable at the 10–20% level for $0.1 < v < 3$. Outside this range, Eq. (*A*.9) overestimates the effective σ.

11.2. Quadrupoles

A photon spectrum integrated over a quadrupole field may be derived from (*A*.4).[56] This spectrum is not very useful for background calculations because only the spectrum hitting the mask is interesting, not the spectrum going down the beampipe. The moments of a quad spectrum may be interesting for power reasons. For a Gaussian beam, the field scale is B_σ, the quad field at 1 σ of the beam. The number of radiated photons and the radiated energy in units of the values for a bend magnet with B_σ are, with b the beam centroid offset in σ units:

Gaussian Beam	Photon Number $\langle n\rangle/n_\sigma$	Radiated Energy U/U_σ
1-D	$\sqrt{(2/\pi)}+b$	$1+b^2$
2-D (round)	$\sqrt{(\pi/2)}$ $(b=0$ only)	$2+b^2$

Table A.2. *Number of radiated photons and the radiated energy in units of the values for a bend magnet with B_σ, with b the beam centroid offset in σ units.*

11.3. Random Sampling from the Synchrotron Radiation Distribution

The nicest routine I know for random sampling from the spectrum Eq. (*A*.4) is due to Yokoya.[57] *RN* is a random number uniform between 0 and 1 representing the integral number distribution between v and infinity. The returned values of v are within 0.05% of Mack's values,[1] at least for $0.001 < v < 12$.

```
  DATA YA1/0.5352 /, YA2/0.3053 /, YA3/0.1418 /, YA4/0.4184 /,
% YB0/0.01192 /, YB1/0.2065 /, YB2/-0.3281 /,
% YC0/0.003314 /, YC1/0.1927 /, YC2/0.8877 /,
% YD0/148.3 /, YD1/675.0 /, YE0/-692.2 /, YE1/-225.5 /

    IF(RN.GT..342)THEN
  P1=1.0-RN
  P2=P1*P1
  V=(((YA4*P2+YA3)*P2+YA2)*P2+YA1)*P2*P1
    ELSEIF(RN.GT.0.0297)THEN
  V=((YB2*RN+YB1)*RN+YB0)/(((RN+YC2)*RN+YC1)*RN+YC0)
    ELSE
  T1=-LOG(RN)
  V=T1+(YD1*T1+YD0)/((T1+YE1)*T1+YE0)
```

11.4. Short-Bend Radiation

A magnet in which the bend angle is less than $1/\gamma$ is called a short magnet; the spectrum does not follow Eq. $(A.4)$ and depends on the z variation of B. The amount of energy is roughly the same as given in Section A.2 above, but the scale or characteristic energy is greater,[54] where with $k_{c-\text{long}}$ given by Eq. $(A.2)$,

$$k_{c-\text{short}} \approx k_{c-\text{long}} \frac{\frac{2}{\gamma}}{\phi} . \qquad (A.10)$$

11.5. General SR Spectrum

The spectrum in Section A.1 is for $k_c \ll E$. The general case is[58,59,60]

$$\frac{1}{n}\frac{dn}{dy} = \frac{3}{5\pi}\frac{1}{(1+\xi y)^2} \times \left[\int_y^\infty K_{5/3}(x)\,dx + \frac{\xi^2 y^2}{1+\xi y} K_{2/3}(y)\right] , \qquad (A.11)$$

$$y = \frac{\frac{k}{k_c}}{1-\frac{k}{E}} = \frac{v}{1-u} = v(1+\xi y) , \qquad (A.12)$$

$$\xi = \frac{k_c}{E} = \frac{3}{2}\Upsilon , \qquad (A.13)$$

where n is given by $(A.1)$, and v only enters in the combination y. For $\xi = 0$, $(A.11)$ reduces to $(A.4)$. Υ is frequently used as a measure of k_c/E rather than ξ.[59,60] For Monte Carlo sampling of $(A.11)$ see Reference 57.

APPENDIX B

NOTATION

a	Radius
b	Radius
c	Velocity of light
f_b	Bunch crossing frequency, $f_b = c/s_b$
k	HOM loss parameter, usually pV/C
k	Photon energy, usually keV
k'	Scattered photon energy
k_c	Characteristic energy of synchrotron radiation
m	Electron mass (energy or momentum, i.e., missing factors of c)
n	Number of radiated SR photons
p	Momentum
q	Bunch charge
q^2	(Momentum transfer)^2
r_e	Classical radius of electron, 2.82×10^{-13} cm
s	Path length along orbit
s_b	Bunch spacing
u	Energy loss normalized to E, e.g., k/E
v	Normalized photon energy, k/k_c
w	Angle nomalized to $1/\gamma$, $w = \gamma\times$ angle
z	Distance along beam axis
A	Atomic weight
B	Magnetic field, usually kG
E	Beam energy
I	Beam current
L	Magnet length, usually m
SR	Synchrotron radiation
T	Kinetic energy
U	Energy radiated
Z	Atomic number
Z_o	377 ohms
α	1/137
γ	E/m
δ	Skin depth, usually μm
μ	RF magnetic permeability relative to vacuum
ϕ	Bend angle
σ	Cross section
σ_z	Rms bunch length, Gaussian parameter
$\sigma(Z)$	DC electrical conductivity of material of atomic number Z
θ	Scattering angle
ρ	Radius of curvature

REFERENCES

1. A. R. Clark (LBL) wrote QSRAD in the early 1970s for use with PEP. Many versions exist now. There is no write-up, as far as I know.
2. W. R. Nelson, H. Hirayama, and D. W. O. Rogers, *The EGS4 Code System*, SLAC Report–265, December 1985. The only approximations in EGS4 that I know of that might affect B Factory calculations are no L-shell fluorescence radiation, no elastic nuclear form factors, and no quasi-elastic or inelastic nucleon/nuclear scattering of any kind.
3. B. Rossi, *High-Energy Particles*, Prentice-Hall, 1952. These formulas may be found in many other places.
4. H. Bethe and J. Ashkin in *Experimental Nuclear Physics*, Vol. 1, ed. E. Segre (Wiley, NY, 1953).
5. H. W. Koch and J. W. Motz, Bremsstrahlung Cross-Section Formulas and Related Data, *Rev. Mod. Phys.* **31**, 920 (1959).
6. D. C. Carey, K. L. Brown, and Ch. Iselin, *DECAY TURTLE*, SLAC–246/UC–28/Fermilab PM–31, March 1982. For beam-gas interactions, we use a version of DECAY TURTLE as modified by W. Kozanecki at SLAC.
7. W. Kozanecki (SLAC), private communication, March 1990.
8. Y.-S. Tsai, Pair Production and Bremsstrahlung of Charged Leptons, *Rev. Mod. Phys.* **46**, 825 (1974); Errata, **49**, 421 (1977).
9. Y. Baconnier, Neutralization of Accelerator Beams by Ionization of the Residual Gas, CERN 85-15, CERN Accelerator School, Gif-sur-Yvette, 1984.
10. C.J. Bocchetta and A. Wrulich, The Trappping and Clearing of Ions in Elletra, *Nucl. Inst. Meth.* **A278**, 807 (1989).
11. V.I. Telnov, Scattering of Electrons on Thermal Radiation Photons in e^+e^- Storage Rings, *Nucl. Inst. Meth.* **A260**, 304 (1987).
12. B. Dehning, *et al.*, Scattering of High Energy Photons off Thermal Photons, *Phys. Lett.* **2349B**, 145 (1990).

13. L. W. Jones and T. O. Dershem, p. 183, *12th Int. Conf. on High-Energy Accelerators*, Fermi National Accelerator Laboratory, 1983.

14. J. W. Lightbody, Jr. and J. S. O'Connel, Modeling single-arm electron scattering and nucleon production from nuclei by GeV electrons, *Computers in Physics*, May/June 1988, p. 57.

15. K. V. Alanakyan *et al.*, On the Angular Dependence of Photoprotons from Nuclei Irradiated with γ-Quanta with Maximum Energy 4.5 GeV, *Nucl. Phys.* **A367**, 429 (1981).

16. K. W. Chen *et al.*, Electroproduction of Protons at 1 and 4 BeV, *Phys. Rev.* **135**, B1030 (1964). These authors deduced an equivalent radiator of about 0.025 radiation lengths.

17. R. D. Evans, *Encyclopedia of Physics*, Vol. XXXIV (Springer-Verlag, Berlin, 1958).

18. A. T. Nelms and I. Oppenheim, Data on the Atomic Form factor: Computation and Survey, *J. Res. Nat. Bureau of Standards* **55**, No. 1, July 1955, pp. 53–62.

19. I. F. Ginzburg, G. L. Kotkin, V. G. Serbo, and V. I. Telnov, Colliding γe and $\gamma\gamma$ Beams Based on the Single-Pass ee Colliders (VLEPP Type), *Nucl. Inst. Meth.* **205**, 47 (1983).

20. J. W. Motz, H. A. Olsen, and H. W. Koch, Pair Production by Photons, *Rev. Mod. Phys.* **41**, 581 (1969). This gives the γe cross section.

21. S. A. Heifets, Photon Beam at CEBAF, CEBAF TN/90/202, January 1990.

22. J. Kirkby (CERN), private communication, April 1990.

23. J. T. Seeman, Observation of the Beam-Beam Interaction, Nonlinear Dynamics Aspects of Particle Accelerators, *Lecture Notes in Physics*, Vol. 247 (Springer-Verlag, Berlin, 1986).

24. YongHo Chin (LBL), private communication, April 1990. The simulation used a code due to K. Yokoya (KEK) and applies to a *PEP*-like machine as described in Feasibility Study for an Asymmetric *B* Factory Based on *PEP*, LBL PUB-5244/SLAC-352/CALT-68-1589, October 1989.

25. M. Sands, The Physics of Electron Storage Rings: An Introduction, SLAC-121, November 1970.

26. G. Decker and R. Talman, Measurement of the Transverse Particle Distribution in the Presence of the Beam-Beam Interaction, *IEEE Trans. Nuc. Sci.*, **NS–30** (4), 2188 (1983).

27. M. K. Sullivan, Synchrotron Radiation Background in the MAC and TPC Vertex Chambers, Univ. Calif. Intercampus Inst. for Research at Particle Accelerators, c/o SLAC, UC–IIRPA–88–01, May 1988.

28. See Feasibility Study for an Asymmetric B Factory Based on *PEP*, LBL PUB–5244/SLAC–352/CALT–68–1589, October 1989.

29. G. von Holtey and D. Ritson, Mini Beam Pipe at the DELPHI Interaction Region, CERN LEP NOTE 614, October 1988.

30. P. Morton and P. Wilson, Energy Loss and Wall Heating for a Gaussian Bunch in a Cylindrical Pipe, SLAC–AATF/79/15, November 1979.

31. A compendium of computer codes useful in accelerator physics is given in *AIP Conf. Proc. 184*, Vol. 2, NY, 1989.

32. J. J. Bisognano, S. A. Heifets, and B. C. Yunn, Loss Parameters for Very Short Pulses, CEBAF–PR–88–005, July 1988.

33. P. B. Wilson, Introduction to Wakefields and Wake Potentials, Physics of Particle Accelerators (Fermilab, 1987; Cornell, 1988), *AIP Conf. Proc. 184*, Vol. 1, NY, 1989.

34. S.A. Heifetz and S.A. Keifets, Coupling Impedance in Modern Accelerators, SLAC-PUB-5297, September 1990. Extensive summary of mainly analytic results. These authors measure k in cm^{-1}. To convert to V/pC multiply by $Z_0 c/4\pi = 1/4\pi\epsilon_0 = 1/1.11 V\mathrm{cm}/pC$.

35. P. B. Wilson, High Energy Linacs: Applications to Storage Ring RF Systems and Linear Colliders, Physics of Particle Accelerators (Fermilab 1981), *AIP Conf. Proc. 87*, NY, 1982.

36. J. D. Jackson, *Classical Electrodynamics*, 2nd ed. (Wiley, 1975). Note: Jackson's k_c is two times larger than Schwinger's.

37. A. F. Harvey, *Microwave Engineering* (Academic Press, NY, 1963).

38. At 10 GHz, type 430 SS has μ about 10. J. Haimson (Haimson Research Corp.), private communication, April 1990.

39. M. Billing, Power Dissipation in the CLEO II Beam Pipe from Beam Heating, unpublished CESR internal note CON 87-6, May 1987; Issues Affecting Single Bunch Current Limits, *B* Factory Workshop Proc., Syracuse University, September 1989.

40. J. Kent, *Procedings of the Workshop on High Luminosity Asymmetric Storage Rings for B Physics*, Report CALT-68-1552, Caltech, April 1989.

41. See articles in Proc. of 5th European Sym. on Semiconductor Detectors, *Nucl. Inst. Meth.* **A288** (1), 1-292 (1990).

42. J. G. Jernigan *et al.*, Performance Measurement of Hybrid PIN Diode Arrays, SLAC-PUB-5211, May 1990; Intl. Industrial Sym. on SSC, Miami Beach, March 1990.

43. S. L. Shapiro *et al.*, Progress Report on Use of Hybrid Silicon PIN Diode Arrays in High Energy Physics, SLAC-PUB-5212, May 1990; *Vth Intl. Conf. on Instrumentation for Colliding Beam Physics*, Novosibirsk, March 1990.

44. J. V. Allaby *et al.*, The MAC Detector, *Nucl. Inst. Meth.* **A281**, 291 (1989).

45. J. Kadyk *et al.*, Anode Wire Aging Tests with Selected Gases, *IEEE Trans. Nuc. Sci.* **37** (2), 478 (1990).

46. J. Va'vra, Aging in Gaseous Detectors, SLAC-PUB-5207, March 1990; *Vth Intl. Conf. on Instrumentation for Colliding Beam Physics*, Novosibirsk, March 1990.

47. H. B. Luna *et al.*, Bremsstrahlung Radiation Effects on Rare Earth Permanent Magnets, *Nucl. Inst. Meth.* **A285**, 349 (1989). (Note typo in Table 3: for 10^8 cm^{-2}, read 10^{18}.)

48. S. Dushman, *Scientific Foundations of Vacuum Technique*, 2nd edition, eds. S. Dushman and J. M. Lafferty (Wiley, NY, 1962).

49. N. B. Mistry, Ultrahigh Vacuum Systems for Storage Rings and Accelerators, Physics of Particle Accelerators (SLAC 1985), *AIP Conf. Proc. 153*, Vol. 2, NY, 1987.

50. O. Groebner *et al.*, Neutral Gas Desorption and Photoelectric Emission from Aluminum Alloy Vacuum Chambers Exposed to Synchrotron Radiation, *J. Vac. Sci. Technol.* **A7** (2), 223 (1989).

51. B. A. Trickett, The ESRF Vacuum System, *Vacuum* **39**, 607 (1988).

52. H. Hartwig and J.S. Koupsidis, A New Approach for Computing Sputter-Ion Pump Characteristics, *J. Vac. Sci. Technol.* 11, 1154 (1974).

53. J. Schwinger, *Phys. Rev.* **75**, 1912 (1949). Only a few of the numerous references dealing with SR are listed.

54. R. Chrien, A. Hofmann, and A. Molinari, *Phys. Reports* **64**, 249 (1980).

55. R. A. Mack, Cambridge Electron Accelerator Report CEAL-1027, February 1966. Although it is not especially difficult to evaluate these SR formulas using modern computation facilities, Mack's report was quite an accomplishment in 1966.

56. E. Keil, Synchrotron Radiation from a Large Electron-Positron Storage Ring, CERN/ISR-LTD/76-23, June 1976.

57. K. Yokoya, A Computer Simulation Code for the Beam-Beam Interaction in Linear Colliders, KEK-Report 85-9, October 1985.

58. K. Yokoya and P. Chen, Electron Energy Spectrum and Maximum Disruption Angle under Multi-Photon Beamstrahlung, SLAC-PUB-4935, March 1989, *IEEE Particle Accelerator Conf.*, Chicago, March 1989.

59. A. A. Sokolov and I. M. Ternov, *Synchrotron Radiation* (Pergamon Press, NY, 1968); *Radiation from Relativistic Electrons* (American Inst. Phys., NY, 1986).

60. T. Erber, High-Energy Conversion Processes in Intense Magnetic Fields, *Rev. Mod. Phys.* **38**, 626 (1966). The spectrum here uses a different, but equivalent, combination of Bessel functions in Eq. (*A*.11).

References

[1] See for example the various presentations on LC Beam Instrumentation at http://www.slac.stanford.edu/xorg/lcd/ipbi/documentation.html, in particular IPBI TN-2003-1.

[2] G. Blaylock *et al.*, SLAC-PUB-5649(January 1992), and references therein.

[3] M. Berndt *et al.*, SLAC-PUB-2289 (March 1979).

[4] Workshop on Physics and Detector Issues for a High Luminosity Asymmetric B Factory at SLAC, January-June 1900, SLAC 373 (March 1991).

[5] LCRD – E. Torrence, "Luminosity, Energy, Polarization" in a Proposal for Linear Collider Research and Development that can be found at http://www.hep.uiuc.edu/LCRD/pdf_docs/LCRD_UCLC_Big_Doc/.